JACS
JOURNAL OF THE AMERICAN CHEMICAL SOCIETY
Communication
pubs.acs.org/JACS

Effective Antisense Gene Regulation via Noncationic, Polyethylene Glycol Brushes

Xueguang Lu, Fei Jia, Xuyu Tan, Dali Wang, Xueyan Cao, Jiamin Zheng, and Ke Zhang*

Department of Chemistry and Chemical Biology, Northeastern University, Boston, Massachusetts 02115, United States

Supporting Information

ABSTRACT: Negatively charged nucleic acids are often complexed with polycationic transfection agents before delivery. Herein, we demonstrate that a noncationic, biocompatible polymer, polyethylene glycol, can be used as a transfection vector by forming a brush polymer-DNA conjugate. The brush architecture provides embedded DNA strands with enhanced nuclease stability and improved cell uptake. Because of the biologically benign nature of the polymer component, no cytotoxicity was observed. This approach has the potential to address several long-lasting challenges in oligonucleotide therapeutics.

Oligonucleotide-based gene therapy holds tremendous promise for treating a variety of disorders with a genetic basis, including cancers, neurological diseases, and metabolic conditions.[1] However, since its conceptualization in the 1970s,[2] there have only been a relatively small number of commercial successes (e.g., Vitravene, Macugen, and Kynamra),[3] despite powerful advancement in the understanding of the underlying biology.[4] This contrast exemplifies the difficulties in transforming nucleic acids to drugs: poor accumulation at target sites, unwanted innate and adaptive immune responses, nuclease degradation, coagulopathy, poor cellular uptake, and overall low biochemical efficacy.[5]

Cationic polymers' ability to complex with nucleic acids and deliver them to cells has been extensively explored as a route to therapeutic intervention.[6] Despite significant progress, however, these materials are still prone to various degrees of cytotoxic and immunogenic reactions, which limit their clinical application.[7] Recently, a new type of nucleic acid nanostructure, termed spherical nucleic acids (SNAs), has emerged as a noncationic, single-entity transfection agent.[8] Consisting of tens to hundreds of oligonucleotide strands densely arranged onto a spherical core, SNAs are capable of entering cells in large quantities despite their negative charge and knocking down target genes without significant cytotoxicity and stimulation of the innate immune system.[9] Due to the dense arrangement, the SNA oligonucleotides are more stable to nuclease degradation than their free, linear counterparts.[10] These observations led us to suspect that the unusual ability of the SNA to act as an antisense agent and its enzyme stability may not be a coincidence. It is possible that enhanced nuclease stability is an important factor for SNAs to survive the endocytotic processing and eventually enter the cytosol to serve their intended purpose.[11] In other words, enhanced nucleic acid stability may be a crucial if not the bottleneck junction in oligonucleotide therapy for noncationic systems.

Inspired by the SNAs, we have developed a novel form of polymer-DNA conjugate, termed polymer-assisted-compaction of DNA (pacDNA), which consists of oligonucleotide (1−3 strands) covalently attached to the backbone of a sterically congested brush polymer with polyethylene glycol (PEG) side chains.[12] By carefully designing the relative lengths of the DNA strands and the PEG side chains, we have shown that the pacDNAs can achieve >20-fold increase in half-life for DNase I, while hybridization with complementary strands remains kinetically unaffected. Therefore, we contemplate that it is possible for the pacDNA to endure the endosome/lysosome environment and, thus, enter the cytosol through normal endosomal processing pathways[13] and regulate gene expression with minimal perturbation to the cell. In contrast, cationic species often cause cell membrane/endosome perforation, leading to toxicity.[14] The use of PEG for oligonucleotide delivery can also improve the biopharmaceutical properties of the oligonucleotide by suppressing unwanted, nonantisense interactions with various proteins.[15] Furthermore, factors previously recognized as important for cocarrier systems such as nucleic acid dissociation from complex and proton buffering capacity do not apply to the pacDNA, thereby simplifying carrier design.[11]

To test our hypothesis, we have designed an antisense pacDNA having 10 kDa PEG side chains that targets the human epidermal growth factor receptor 2 (Her2) mRNA ($pacDNA_{10k}$, Scheme 1). Her2 is an important biomarker for many cancers including several types of breast and ovarian cancers,[16] and antisense control of the Her2 gene has been previously demonstrated.[17] For controls, we use an improper pacDNA with overly short side chains (5 kDa), and a Y-shaped PEG-DNA conjugate ($_{Y}$PEG-DNA). The $pacDNA_{5k}$ is incapable of effectively protecting the embedded DNA against enzymatic degradation (*vide infra*). The $_{Y}$PEG is routinely used to form bioconjugates and is found in commercial oligonucleotide drug formulations (Macugen).[18] However, because of the low density of the PEG chains (2 chains), adequate enzymatic protection to the DNA is not anticipated.

Previously, the pacDNA structure was synthesized by coupling amine-modified DNA to diblock brush polymer containing *N*-hydroxyl succininimide (NHS) groups in an aqueous bicarbonate buffer. The reaction efficiency is affected by the hydrolysis of NHS groups, requiring the use of large

Received: June 6, 2016
Published: July 15, 2016

DOI: 10.1021/jacs.6b05787
J. Am. Chem. Soc. 2016, 138, 9097−9100

Scheme 1. Structures of pacDNA and Y-Shaped PEG-DNA Conjugate

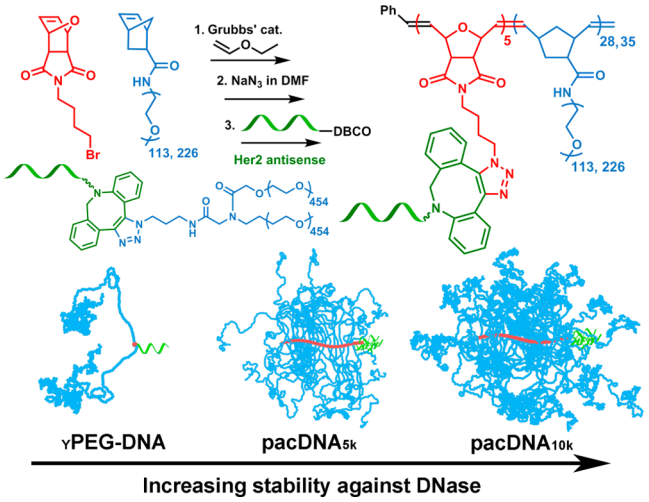

excesses (>20:1 mol:mol) of the DNA. In this study, cyclooctyne-mediated copper-free click chemistry[19] replaces the amidation reaction, resulting in near-quantitative yields. To achieve the coupling, the Her2 antisense DNA strand is modified with 5′ dibenzocyclooctyne (DBCO) group (sequence: 5′ DBCO CTC CAT GGT GCT CAC TTT 3′), while the brush polymer bears the azide groups. The brush polymers are synthesized via sequential ring opening metathesis polymerization (ROMP) of norbornenyl bromide (N-Br) and norbornenyl PEG (N-PEG, M_n = 5 or 10 kDa, PDI < 1.05), followed by azide substitution of the bromide.[20] The resulting brush is of a diblock structure, with the first, oligomeric block (~5 repeating units) serving as a reactive region for DNA conjugation and the second, longer block (~30 repeating units) creating the brush architecture and the steric congestion needed to protect the DNA. Dimethylformamide gel permeation chromatography shows narrow molecular weight distribution (PDI < 1.15) for the brush polymers (Table 1 and Figure S1; polystyrene-equivalent MW is shown), and the successful incorporation of the azide group is verified by infrared spectroscopy, which shows characteristic vibration of the azido group at 2029 cm^{-1} (Figure S2).[21]

Table 1. GPC Analyses for the Brush Polymers Used

polymer	composition	M_n (kDa)	M_w (kDa)	PDI
$brush_{5k}$	pN-$azide_5$-*b*-pN-$PEG(5k)_{35}$	178.8	197.2	1.10
$brush_{10k}$	pN-$azide_5$-*b*-pN-$PEG(10k)_{28}$	285.5	329.1	1.15

Coupling of the DBCO-modified DNA strand to the brush polymers and the $_Y$PEG is achieved by incubation in 2 M NaCl solution at 40 °C for 48 h (3:1 alkyne:azide mol:mol). The elevated salt concentration is required to achieve high DNA loading by screening the charge between DNA strands. Purified conjugates are free of unconjugated DNA as shown by aqueous GPC and agarose gel electrophoresis (Figures 1A and S3). The numbers of DNA strands per brush was determined by peak integration of the GPC chromatograms recorded at 488 nm to be 5.7 and 4.9 for $pacDNA_{10k}$ and $pacDNA_{5k}$, respectively (Figure S4). The pacDNAs exhibit a spherical morphology, with a dry-state diameter of 18.2 ± 2.5 for $pacDNA_{5k}$ and 21.9 ± 3.1 nm for $pacDNA_{10k}$, as evidenced by transmission electron microscopy (TEM) (Figures 1E,F and S5). These measurements are consistent with dynamic light scattering analysis, showing number-average hydrodynamic diameters of 17.0 ± 4.2 and 23.7 ± 5.9 nm for the 5k and 10k pacDNAs, respectively (Figure 1C and D). Zeta potential measurements indicate that pacDNAs and the $_Y$PEG-DNA have significantly reduced negative surface charge (from −9.8 to −20.3 mV) compared with free DNA in nanopure water (−47.4 mV, Figure 1B), which is expected from the dilution of surface charge for the conjugates.

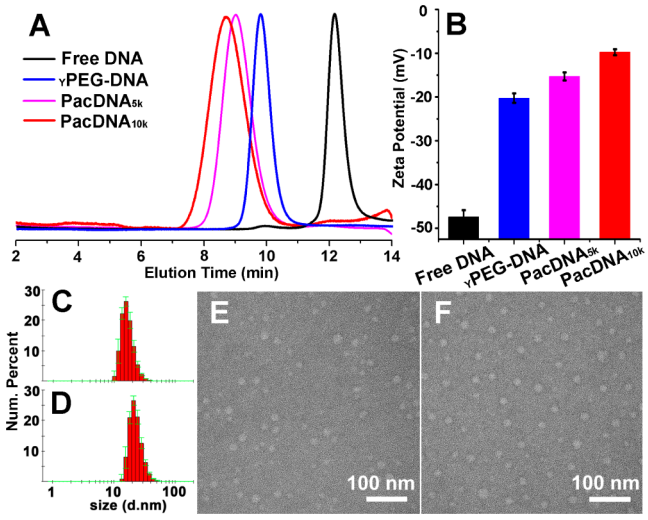

Figure 1. (A) Aqueous GPC chromatograms and (B) zeta potential measurements of free DNA, $_Y$PEG-DNA, $pacDNA_{5k}$, and $pacDNA_{10k}$. (C–F) Number-average hydrodynamic diameter distributions for $pacDNA_{5k}$ (C) and $pacDNA_{10k}$ (D), and corresponding TEM images (E–F, images are negatively stained with uranyl acetate).

We next compare the ability of the DNA conjugates to hybridize with complementary strands and resist nuclease degradation. Hybridization is monitored by a fluorescence quenching assay, where a quencher (dabcyl)-modified complementary strand is added to fluorescein-labeled conjugates. The rate of fluorescence decrease is a direct indicator of the hybridization kinetics (Figure 2A). Remarkably, both pacDNAs and the $_Y$PEG-DNA hybridize rapidly with complementary DNA ($t_{1/2}$ < 10 s), with negligible difference compared with free DNA (Figure 2B). When a dummy (noncomplementary) dabcyl-DNA strand is added, fluorescence intensities are not

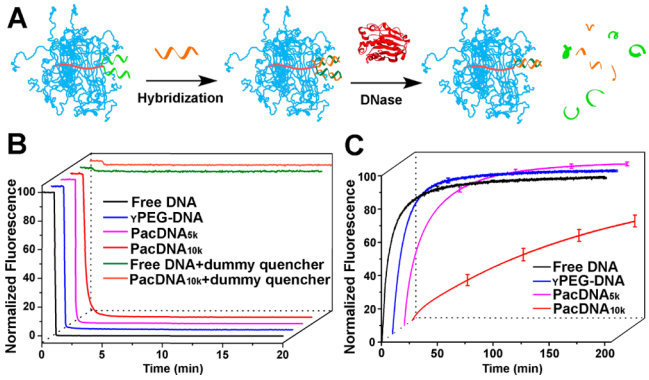

Figure 2. (A) Schematics of DNA hybridization and DNase I degradation assays. (B–C) Hybridization and degradation kinetics of pacDNAs, $_Y$PEG-DNA, and free DNA.

DOI: 10.1021/jacs.6b05787
J. Am. Chem. Soc. 2016, 138, 9097–9100

affected, ruling out nonhybridization interactions. In order to probe the extent of nuclease protection, DNase I is added to fluorescein-labeled DNA conjugates that are prehybridized to dabcyl-modified complementary strands. Upon DNase I action, the fluorophore is released, which leads to an increase of fluorescence (Figure 2A). The pacDNA$_{10k}$ exhibits significantly extend half-life ($t_{1/2}$) of ~141.9 min compared with free DNA, which is degraded rapidly with a $t_{1/2}$ 0f ~ 6.0 min (Figure 2C and Table S2). On the other hand, pacDNA$_{5k}$ has very limited protective power, showing a $t_{1/2}$ of ~13.2 min. This is not surprising because the fluorophore is located at the periphery (3′) of the DNA; once the DNA extends beyond the PEG shell of the brush, the exposed portion should experience a rapid drop-off in steric protection. Similarly, the $_{Y}$PEG barely lends any protection to conjugated DNA, with a $t_{1/2}$ of ~8.2 min, despite having twice the length of the side chains of pacDNA$_{10k}$. These results suggest that both the brush side chain length and steric congestion created by a densely grafted architecture are critical to providing oligonucleotides with steric selectivity.

In order for the pacDNA to serve as an antisense agent, it needs to efficiently enter cells. We evaluated the cell uptake efficiency in SKOV3, a human ovarian cancer line. To enable tracking, conjugates are labeled at the DNA component with the fluorophore Cy3. Cells are incubated with the conjugates and free DNA for 6 h, followed by flow cytometry analysis. Interestingly, cell uptake appears to be a function of DNA accessibility; the better hidden the DNA, the greater the cell uptake (Figure 3C). This is an advantageous phenomenon

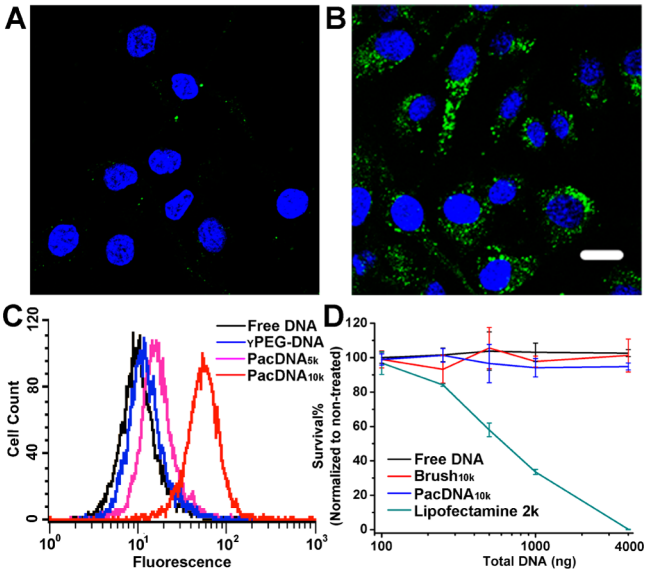

Figure 3. Confocal fluorescence microscopy images of SKOV3 cells incubated with 100 nM of free Cy3-DNA (A) or Cy-3 pacDNA$_{10k}$ (B). Cell nuclei were stained with DAPI (blue). Scale bar is 20 μm. (C) Flow cytometry measurements of cells treated with 100 nM Cy3-labeled samples. (D) MTT cytotoxicity assay for SKOV3 cells.

because DNA accessibility is inversely correlated with nuclease stability. Confocal microscopy confirms the cell uptake of the pacDNA. As shown in the Figures 3A,B and S6, free DNA-treated cells produce a very small amount of fluorescence signals, while the same concentration of DNA, when packaged into pacDNA$_{10k}$, results in much stronger fluorescence signals under identical imaging settings. Quantification using cell lysates shows that there are ~7.7 × 10^5 pacDNA$_{10k}$ particles/cell when the cells are incubated with an equivalent of 1 μM of DNA for 6 h (Figure S7). While the pacDNA clearly improves DNA uptake, the extent of uptake is still much below that of the SNA, for which the number of particles/cell often exceeds 10^6 when similar DNA concentrations (~10 nM SNA) are used.[22]

Having demonstrated that the pacDNA has improved cell uptake, we next studied its antisense activity toward Her2 in SKOV3 cells, which is a Her2-overexpressing cell line. For positive controls, Lipofectamine, an effective cationic liposomal transfection agent, and SNAs with 13 nm gold nanoparticle cores bearing identical antisense strands are used. PacDNA$_{10k}$ containing a scrambled sequence (scr-pacDNA$_{10k}$) and brush polymers devoid of DNA strands are used as negative controls. We verified that scr-pacDNA$_{10k}$ exhibits similar levels of cell uptake and resistance to DNase I as the pacDNA$_{10k}$ bearing the antisense sequence (Figures S8 and S9). SKOV3 cells were treated with samples and controls at varying concentrations (10−1000 nM DNA) for 20 h, followed by culturing for another 48 h in fresh media. The total cellular protein for each sample is harvested and analyzed by Western blot. It is found that the Her2 levels are significantly reduced by pacDNA$_{10k}$, SNA, and Lipofectamine-complexed DNA (Figure 4). Strik-

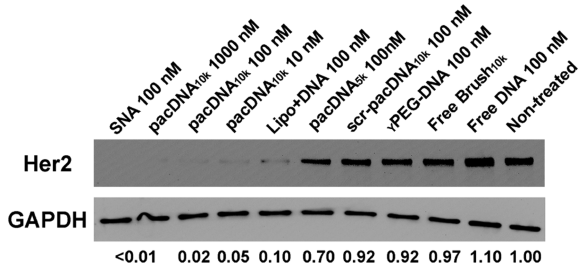

Figure 4. Western blot analysis of pacDNAs and controls. Her2 expression reduction was observed for pacDNA$_{10k}$, Lipofectamine, and SNA, while pacDNA$_{5k}$ and $_{Y}$PEG-DNA did not show significant antisense activity.

ingly, even at a low concentration (10 nM), the pacDNA$_{10k}$ was able to reduce Her2 expression to only 5% of untreated, as determined by band densitometry analysis, while scrambled pacDNA$_{10k}$ does not reduce Her2 expression. On the other hand, pacDNA$_{5k}$, $_{Y}$PEG-DNA, and free DNA show no Her2 expression reduction compared with untreated cells. These data corroborate our hypothesis that DNA stability plays an important role in noncationic gene regulation; only adequately protected oligonucleotides are able to withstand the digestive endosomal processing and perform downstream action. Unprotected nucleic acids are efficiently cleaved and deactivated by the cells. Because pacDNA consists of nontoxic components (PEG and DNA), we anticipate its cytotoxicity to be minimum. Indeed, MTT cytotoxicity assays for SKOV3 and 4T1 cells show essentially no cytotoxicity at 4000 ng of DNA, the highest concentration tested (Figures 3D and S10), while Lipofectamine results in significant cell death (>50%) above 400 ng of DNA.

In summary, our data suggest that efficient cell uptake and enhanced oligonucleotide stability is a successful combination for noncationic gene regulation; facilitated endosomal release by a membrane-disrupting agent is not required. The pacDNA have desired characteristics to make it an ideal noncationic oligonucleotide delivery platform, thanks to the densely

DOI: 10.1021/jacs.6b05787
J. Am. Chem. Soc. 2016, 138, 9097−9100

arranged side chains of the brush and the biocompatibility of PEG. Because of its ability to shield DNA from proteins and bypass serum opsonization, the pacDNA has the potential to be applied *in vivo* for many oligonucleotide-based applications.

■ ASSOCIATED CONTENT

Supporting Information

The Supporting Information is available free of charge on the ACS Publications website at DOI: 10.1021/jacs.6b05787.

Materials, experimental procedures, instrumentation and supplemental figures (PDF)

■ AUTHOR INFORMATION

Corresponding Author

*k.zhang@neu.edu

Notes

The authors declare no competing financial interest.

■ ACKNOWLEDGMENTS

We thank Prof. George O'Doherty for support with cell culture. Financial support from Northeastern University start-up, NEU-DFCI seed grant, and NSF CAREER award (1453255) is gratefully acknowledged.

■ REFERENCES

(1) (a) Hyde, S. C.; Gill, D. R.; Higgins, C. F.; Trezise, A. E.; MacVinish, L. J.; Cuthbert, A. W.; Ratcliff, R.; Evans, M. J.; Colledge, W. H. *Nature* **1993**, *362*, 250. (b) Simonato, M.; Bennett, J.; Boulis, N. M.; Castro, M. G.; Fink, D. J.; Goins, W. F.; Gray, S. J.; Lowenstein, P. R.; Vandenberghe, L. H.; Wilson, T. J.; Wolfe, J. H.; Glorioso, J. C. *Nat. Rev. Neurol.* **2013**, *9*, 277. (c) Aiuti, A.; Cattaneo, F.; Galimberti, S.; Benninghoff, U.; Cassani, B.; Callegaro, L.; Scaramuzza, S.; Andolfi, G.; Mirolo, M.; Brigida, I.; Tabucchi, A.; Carlucci, F.; Eibl, M.; Aker, M.; Slavin, S.; Al-Mouse, H.; Al Ghonaium, A.; Ferster, A.; Duppenthaler, A.; Notarangelo, L.; Wintergerst, U.; Buckley, R. H.; Bregni, M.; Martkel, S.; Valsecchi, M. G.; Rossi, P.; Ciceri, F.; Miniero, R.; Bordignon, C.; Roncarolo, M. G. *N. Engl. J. Med.* **2009**, *360*, 447.

(2) (a) Stephenson, M. L.; Zamecnik, P. C. *Proc. Natl. Acad. Sci. U. S. A.* **1978**, *75*, 285. (b) Rayburn, E. R.; Zhang, R. *Drug Discovery Today* **2008**, *13*, 513.

(3) Aartsma-Rus, A. *Mol. Ther.* **2016**, *24*, 193.

(4) Winter, J.; Jung, S.; Keller, S.; Gregory, R. I.; Diederichs, S. *Nat. Cell Biol.* **2009**, *11*, 228.

(5) (a) Verma, I. M.; Somia, N. *Nature* **1997**, *389*, 239. (b) Gabrielson, N. P.; Lu, H.; Yin, L.; Li, D.; Wang, F.; Cheng, J. *Angew. Chem.* **2012**, *124*, 1169.

(6) (a) Zhang, K.; Fang, H.; Wang, Z.; Taylor, J.-S. A.; Wooley, K. L. *Biomaterials* **2009**, *30*, 968. (b) Lächelt, U.; Wagner, E. *Chem. Rev.* **2015**, *115*, 11043. (c) Chen, C.; Law, W.; Aalinkeel, R.; Yu, Y.; Nair, B.; Wu, J.; Mahajan, S.; Reynold, J. L.; Li, Y.; Lai, C. K.; Tzanakakis, E. S.; Schwartz, S. A.; Prasad, P. N.; Cheng, C. *Nanoscale* **2014**, *6*, 1567. (d) Liu, G.; Swierczewska, M.; Lee, S.; Chen, X. *Nano Today* **2010**, *5*, 524.

(7) (a) Miller, A. D. *Curr. Med. Chem.* **2003**, *10*, 1195. (b) Li, S.; Huang, L. *Gene Ther.* **2000**, *7*, 31.

(8) (a) Mirkin, C. A.; Letsinger, R. L.; Mucic, R. C.; Storhoff, J. J. *Nature* **1996**, *382*, 607. (b) Cutler, J. I.; Auyeung, E.; Mirkin, C. A. *J. Am. Chem. Soc.* **2012**, *134*, 1376.

(9) (a) Rosi, N. L.; Giljohann, D. A.; Thaxton, C. S.; Lytton-Jean, A. K. R.; Han, M. S.; Mirkin, C. A. *Science* **2006**, *312*, 1027. (b) Rush, A. M.; Nelles, D. A.; Blum, A. P.; Barnhill, S. A.; Tatro, E. T.; Yeo, G. W.; Gianneschi, N. C. *J. Am. Chem. Soc.* **2014**, *136*, 7615. (c) Chen, T.; Wu, C. S.; Jimenez, E.; Zhu, Z.; Dajac, J. G.; You, M.; Han, D.; Zhang, X.; Tan, W. *Angew. Chem.* **2013**, *125*, 2066.

(10) (a) Rush, A. M.; Thompson, M. P.; Tatro, E. T.; Gianneschi, N. C. *ACS Nano* **2013**, *7*, 1379. (b) Seferos, D. S.; Prigodich, A. E.; Giljohann, D. A.; Patel, P. C.; Mirkin, C. A. *Nano Lett.* **2009**, *9*, 308. (c) Tan, X.; Li, B. B.; Lu, X.; Jia, F.; Santori, C.; Menon, P.; Li, H.; Zhang, B.; Zhao, J. J.; Zhang, K. *J. Am. Chem. Soc.* **2015**, *137*, 6112.

(11) Zhao, F.; Zhao, Y.; Liu, Y.; Chang, X.; Chen, C.; Zhao, Y. *Small* **2011**, *7*, 1322.

(12) Lu, X.; Tran, T.-H.; Jia, F.; Tan, X.; Davis, S.; Krishnan, S.; Amiji, M. M.; Zhang, K. *J. Am. Chem. Soc.* **2015**, *137*, 12466.

(13) Grant, B. D.; Donaldson, J. G. *Nat. Rev. Mol. Cell Biol.* **2009**, *10*, 597.

(14) Sovadinova, I.; Palermo, E. F.; Huang, R.; Thoma, L. M.; Kuroda, K. *Biomacromolecules* **2011**, *12*, 260.

(15) Ikeda, Y.; Nagasaki, Y. *J. Appl. Polym. Sci.* **2014**, *131*, 40293.

(16) (a) Mitri, Z.; Constantine, T.; O'Regan, R. *Chemother. Res. Pract.* **2012**, *2012*, 743193. (b) Verri, E.; Guglielmini, P.; Puntoni, M.; Perdelli, L.; Papadia, A.; Lorenzi, P.; Rubagotti, A.; Ragni, N.; Boccardo, F. *Oncology* **2005**, *68*, 154.

(17) (a) Vaughn, J. P.; Iglehart, J. D.; Demirdji, S.; Davis, P.; Babiss, L. E.; Caruthers, M. H.; Marks, J. R. *Proc. Natl. Acad. Sci. U. S. A.* **1995**, *92*, 8338. (b) Zhang, K.; Hao, L.; Hurst, S. J.; Mirkin, C. A. *J. Am. Chem. Soc.* **2012**, *134*, 16488.

(18) Ng, E. W.; Shima, D. T.; Calias, P.; Cunningham, E. T.; Guyer, D. R.; Adamis, A. P. *Nat. Rev. Drug Discovery* **2006**, *5*, 123.

(19) Zhang, C.; Macfarlane, R. J.; Young, K. L.; Choi, C. H. J.; Hao, L.; Auyeung, E.; Liu, G.; Zhou, X.; Mirkin, C. A. *Nat. Mater.* **2013**, *12*, 741.

(20) (a) Gao, A. X.; Liao, L.; Johnson, J. A. *ACS Macro Lett.* **2014**, *3*, 854. (b) Gutekunst, W. R.; Hawker, C. J. *J. Am. Chem. Soc.* **2015**, *137*, 8038.

(21) Singh, K. S.; Svitlyk, V.; Mozharivskyj, Y. *Dalton Trans.* **2011**, *40*, 1020.

(22) Giljohann, D. A.; Seferos, D. S.; Patel, P. C.; Millstone, J. E.; Rosi, N. L.; Mirkin, C. A. *Nano Lett.* **2007**, *7*, 3818.

DOI: 10.1021/jacs.6b05787
J. Am. Chem. Soc. 2016, 138, 9097–9100